



# Theoretical study of fast diffusion in carbon nanotubes

Cite as: J. Appl. Phys. **128**, 184302 (2020); <https://doi.org/10.1063/5.0031023>

Submitted: 28 September 2020 . Accepted: 25 October 2020 . Published Online: 10 November 2020

 Douglas A. Barlow, and  Fenner E. Colson



View Online



Export Citation



CrossMark

Meet the Next Generation  
of Quantum Analyzers

And Join the Launch  
Event on November 17th



Register now



Zurich  
Instruments



# Theoretical study of fast diffusion in carbon nanotubes

Cite as: J. Appl. Phys. 128, 184302 (2020); doi: 10.1063/5.0031023

Submitted: 28 September 2020 · Accepted: 25 October 2020 ·

Published Online: 10 November 2020



View Online



Export Citation



CrossMark

Douglas A. Barlow<sup>1,a)</sup>  and Fenner E. Colson<sup>2,b)</sup> 

## AFFILIATIONS

<sup>1</sup>Department of Physics and Astronomy, Jacksonville University, Jacksonville, Florida 32211, USA

<sup>2</sup>Department of Chemistry and Physics, Florida Gulf Coast University, Ft. Myers, Florida 33965, USA

**Note:** This paper is part of the Special Topic on Physics and Applications of Nanotubes.

**<sup>a)</sup>Also at:** Alderman Barlow Labs, Trenton, FL 32693, USA. **Author to whom correspondence should be addressed:**

[doug.barlow@aldermanbarlow.com](mailto:doug.barlow@aldermanbarlow.com)

**<sup>b)</sup>**[fcolson@fgcu.edu](mailto:fcolson@fgcu.edu)

## ABSTRACT

Using a recently reported method for the statistical representation of gaseous diffusion within a cylindrical pore, we report here on an analysis of situations that describe fast diffusion within carbon nanotubes. It is proposed that if gaseous flow properties of the tube, in the highly rarefied situation, are due to there being only specular particle-wall reflections, then these particles can transit the tube via self-diffusion. On comparing this self-diffusive flux with Knudsen transport diffusion, our model predicts that enhanced diffusion is indeed possible in the carbon nanotube. Depending upon the statistical nature of the particle-wall scattering phenomenon, the enhancements are predicted to be three to four times that of classical transport diffusion and, for certain conditions, the enhancement factor can be greater than 4.

Published under license by AIP Publishing. <https://doi.org/10.1063/5.0031023>

## I. INTRODUCTION

An important molecular dynamics (MD) study in 2002 predicted that the flow of gaseous particles through carbon nanotubes could be three to four times greater than through zeolite based nanotube systems.<sup>1</sup> This flow enhancement phenomenon has been referred to as *fast diffusion*. Holt *et al.*<sup>2</sup> have reported that for the airflow through carbon nanotube membranes, a flow enhancement of 16–120 times that of the classical Knudsen diffusion prediction occurred. Reliable and well characterized carbon nanotube membranes have since been fabricated by many groups.<sup>3–8</sup>

It has been proposed that this enhanced diffusion within carbon nanotubes is due primarily to the frictionless nature of the pore wall.<sup>9–11</sup> That is, the gaseous particle undergoes primarily specular interactions with the inner surface of the pore.

Recently, Colson and Barlow reported on a statistical method whereby the gaseous flux and a Fickian diffusion coefficient, can be estimated for the gaseous flow within a nanotube.<sup>12</sup> This method conveniently models the flow in terms of a probability distribution for scattering path lengths. In this paper, we report on work where this model is used to examine the nature of the fast diffusion

phenomenon by comparing the flux through a cylindrical carbon nanotube with an identically shaped non-carbon nanotube.

Assuming that fast diffusion in carbon nanotubes is due to particles scattering specularly from the pore walls, we consider here the case where diffusion is solely that of *self-diffusion* with no concentration gradient present. That is, mass transmission within the nanotube can behave in a similar fashion to that of light transmission in a fiber optic cable; the inherent natural motion of the particle generates transport within the conduit. Therefore, propagation is not due to a mass density gradient but rather due to the Brownian thermal motion that initially propelled the particle into the nanotube.

We derive expressions for the carbon nanotube flux, in the highly rarefied situation, for the self-diffusion case. The non-carbon based nanotube system is assumed to exhibit the classical Knudsen *transport diffusion*, where the particle-wall interaction is perfectly diffuse and a concentration gradient is present in the nanotube.<sup>13</sup>

The issue of flow enhancement in carbon based systems is studied by comparing the ratio of the flux in the carbon nanotube to that of a non-carbon system. We consider two cases. In the first case, the distribution for scattering path lengths in both systems is given by a Gaussian distribution. In the second case, the path length

spectrum for the carbon nanotube is assumed to be determined by the trajectory of the particles upon entry while in the non-carbon system diffuse scattering conditions are modeled by a cosine square law.

When using a Gaussian model for the path length distribution, we are able to examine what effect the standard deviation has on the flow enhancement. This analysis reveals a flow enhancement of three to four as the standard deviation broadens, which agrees with the above mentioned MD study.<sup>1</sup> But for a distribution dominated by short path lengths, an anomalous region develops where the enhancement factor strongly diverges to higher values. In the second case, where the path length distribution functions are customized for each nanotube, we are led to a result that gives the enhancement factor in terms of the nanotube length. Here, for lengths typical of those reported for carbon nanotubes, the enhancement ranges from a factor of 3 to 6.

## II. FLUX ENHANCEMENT: THE GAUSSIAN DISTRIBUTION

In the case of the highly rarefied regime, where particle-particle interactions are negligible, Eq. (19) of Ref. 12 expresses the flux,  $J$ , in terms of an integral

$$J = \xi \int_{z_0}^{\infty} [n(2z_0 - z) - n(z)]C(z, z_0)dz, \quad (1)$$

where  $\xi$  is the particle-wall collision frequency,  $n$  is the gaseous density within the tube, and  $C$  is the cumulative probability distribution function for particle-wall axial scattering path lengths. The axial coordinate in the tube is  $z$ . The density  $n$  depends solely on the axial coordinate  $z$ . A flux plane, having the circular cross section of the tube, is located at  $z_0$ . The integral includes contributions from both left and right moving particles. Particles are assumed to be characterized as moving at the same mean velocity and thus with identical translational energies.

If the flux plane is placed at the origin of the coordinate system, then  $C$  is related to the normalized probability function  $P$  for axial scattering path lengths  $\lambda$  as

$$C = \int_z^{\infty} P(\lambda)d\lambda. \quad (2)$$

More generally,  $C$  would be a two-part piecewise expression; one for the right moving flux within the pore and the other for the leftward. However, if both flux contributions are assumed to obey the same distribution function, then this symmetry leads to  $C$  being given by one expression as in Eq. (1).<sup>12</sup>

In this study, we assume that there is gas to the left side of the porous membrane, while at the opposite end, there is vacuum. This situation is depicted below in Fig. 1.

In the self-diffusion case, a particle will enter the pore on the left due to the Brownian thermal motion, undergo a series of specular reflections, and exit at the right end of the pore.

Once the steady-state self-diffusive situation is reached, flow through the pore will occur with a constant gas density of  $n_0$  within the pore.

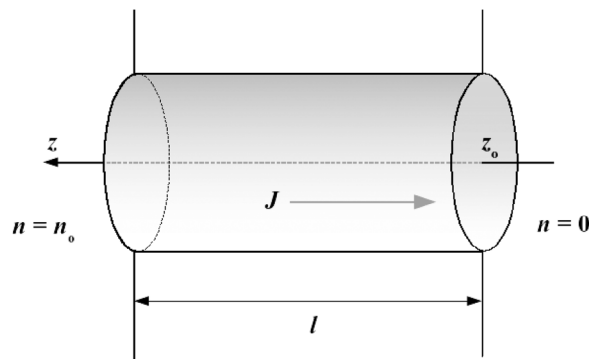


FIG. 1. Depiction of a carbon nanotube in a membrane. The gas density on the left is  $n_0$  while on the right side  $n \approx 0$ . Specular reflection leads to the self-diffusive flux  $J$  which flows from left to right in the figure. Since there is no leftward moving component of the flux, the flux plane located at  $z_0$ , is placed at the right end of the pore.

Let the flux from the specular self-diffusion situation be given by  $J$ . Since there is only rightward moving flux, we have that  $n(2z_0 - z) = 0$  in Eq. (1) leading to

$$J = -\xi \int_{z_0}^{\infty} n(z_0)C(z, z_0)dz. \quad (3)$$

Here,  $n = n_0$ , and the flux plane is set to be at the right end of the pore. Setting  $n(z_0) = n_0$ , using Eq. (2) for  $C$ , and considering a pore of length  $l$  transforms Eq. (3) into

$$J = -\xi n_0 \int_0^l \left( \int_z^{\infty} P(\lambda)d\lambda \right) dz. \quad (4)$$

Equation (1) can also be used to give the flux  $J'$  for Knudsen transport diffusion in the non-carbon nanotube. In this case, due to diffuse scattering, there will be right and leftward moving components of the flux so that both of the density terms, within the square brackets of Eq. (1), survive. Here,  $n = (dn/dz)z + n_0$  with  $dn/dz$  being constant,  $n_0$  being the density at the flux plane, and  $l$  being the membrane thickness. Using this expression for the density in Eq. (1), Colson and Barlow derive Eq. (40) in Ref. 12 for a nanotube of finite length with the flux plane placed at the center of the tube which is

$$J' = -2\xi \frac{dn}{dz} \int_0^{l/2} z \left( \int_z^{\infty} P(\lambda)d\lambda \right) dz. \quad (5)$$

Now, we consider the ratio of specular self-diffusion to Knudsen transport diffusion,

$$\frac{J}{J'} = \frac{-\xi n_0 \int_0^l \left( \int_z^{\infty} P(\lambda)d\lambda \right) dz}{-2\xi \frac{dn}{dz} \int_0^{l/2} z \left( \int_z^{\infty} P(\lambda)d\lambda \right) dz}. \quad (6)$$

The two nanotubes we compare have identical diameters so that

the collision frequencies in Eqs. (4) and (5) are assumed to be equivalent. Letting  $dn/dz = n_0/l$ , the above reduces to

$$\frac{J}{J'} = \frac{l \int_0^l (\int_z^\infty P(\lambda) d\lambda) dz}{2 \int_0^{l/2} z (\int_z^\infty P(\lambda) d\lambda) dz} \tag{7}$$

As a model for  $P$ , we consider the Gaussian distribution normalized over half space with standard deviation  $\sigma$ ,

$$P(\lambda) = \frac{2}{\sqrt{2\pi}\sigma} e^{-\frac{\lambda^2}{2\sigma^2}} \tag{8}$$

Inserting Eq. (8) into Eq. (7) and computing the integrals, we arrive at

$$\frac{J}{J'} = \frac{4l^2 + 4l\sigma\sqrt{\frac{2}{\pi}}(1 - e^{-l^2/2\sigma^2}) - 4l^2 \operatorname{erf}\left[\frac{l}{\sqrt{2}\sigma}\right]}{l^2 - l\sigma\sqrt{\frac{2}{\pi}}e^{-l^2/8\sigma^2} - (l^2 - 4\sigma^2) \operatorname{erf}\left[\frac{l}{\sqrt{2}\sigma}\right]} \tag{9}$$

where erf denotes the error function. Now, the ratio can be studied as a function of  $\sigma$ . Setting  $l = 1$ ,  $\sigma$  is given in the units of the pore length  $l$ .

In Fig. 2, a plot of Eq. (9) is shown. Using a dashed vertical line, we divide the space into two regions. Region II we label as the *fast diffusion* region. In this region, enhancements over transport Knudsen diffusion of three to four times are possible. In fact, one finds that  $\lim_{\sigma \rightarrow \infty} J/J' = 4$ . Values in this region are consistent with the results reported in Ref. 1.

We label region I the *anomalous fast diffusion* region. Here, the ratio  $J/J'$  can assume any positive value greater than 3. However, this is due to the fact that Knudsen transport diffusion falls to zero faster than the self-diffusion. For either diffusion mode in this region, the flux would be limited.

The regions are defined by the relation between the standard deviation of the scattering path length and the pore length. From Fig. 2, we see that when  $\sigma < 0.4l$ , the ratio  $J/J'$  begins to climb

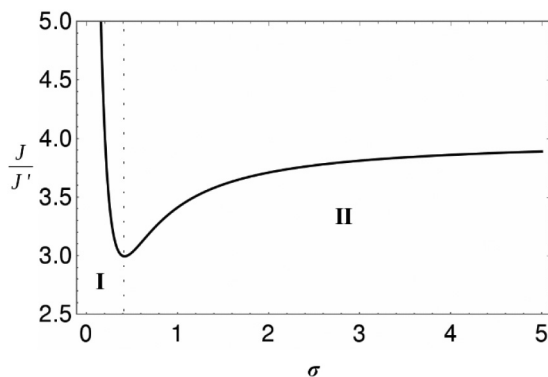


FIG. 2. A plot of the ratio of fluxes given by Eq. (9). The vertical dashed line divides the ratio of fluxes into two regions: II: fast diffusion and I: anomalous fast diffusion.  $\sigma$  has units of pore length  $l$ .

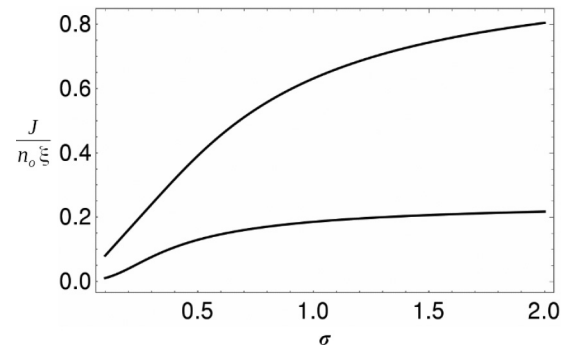


FIG. 3. Normalized flux vs standard deviation in each nanotube for the situation depicted in Fig. 2. The upper curve represents the estimated flux in the carbon nanotube via self-diffusion. The lower curve gives the flux through the non-carbon system due to transport diffusion.  $\sigma$  has units of pore length  $l$ .

considerably. The situation would be that the path length spectrum is dominated by short axial path lengths. In region II where  $\sigma > 0.4l$ , the path length spectrum becomes more spread out, and thus, there are increasingly more long scattering path lengths present in the spectrum. More specifically, when the enhancement factor is 3, and  $\sigma \approx 0.4l$ , the majority of the particles undergo multiple wall collisions within the pore. As the enhancement factor increases toward 4, an increasing fraction of the particles transits the tube having only one particle-wall collision.

To consider region I more closely, a plot showing each flux from Eq. (9) individually is given in Fig. 3. Here, it can be seen that as the standard deviation falls to 0.1 times the pore length, the transport diffusion flux essentially vanishes, while the self-diffusion flux remains finite thus leading to the diverging nature of the ratio within region I.

### III. FLUX ENHANCEMENT: CUSTOM DISTRIBUTIONS

In Sec. II, it was assumed that scattering in both nanotubes could be described by the same path length distribution function. However, since scattering within the carbon nanotube is taken to be specular in nature, we will in this section let the distribution function for scattering path lengths in the carbon nanotube to be based upon the trajectory of the particles upon tube entry. For the non-carbon based system, the distribution will be given the classic cosine squared dependence often used to model diffuse scattering.

As in Sec. II, a self-diffusion model will be used to describe the flux for the carbon nanotube, while for the non-carbon system, transport diffusion will be the transfer mode.

Since the carbon nanotube is taken to yield only specular interactions, we will assume that the path length distribution is determined by the trajectory of the particle upon entry into the tube. Following the work by Turner *et al.*,<sup>14</sup> where the trajectories of atoms sputtered from one flat plate to another were studied, the normalized distribution upon entry is taken to be proportional to  $\cos \theta \sin \theta$ , where  $\theta$  is the angle from the axial of the tube as shown in Fig. 4(a). Here, we will use a more mathematically convenient form of this distribution that retains the main features of the above,

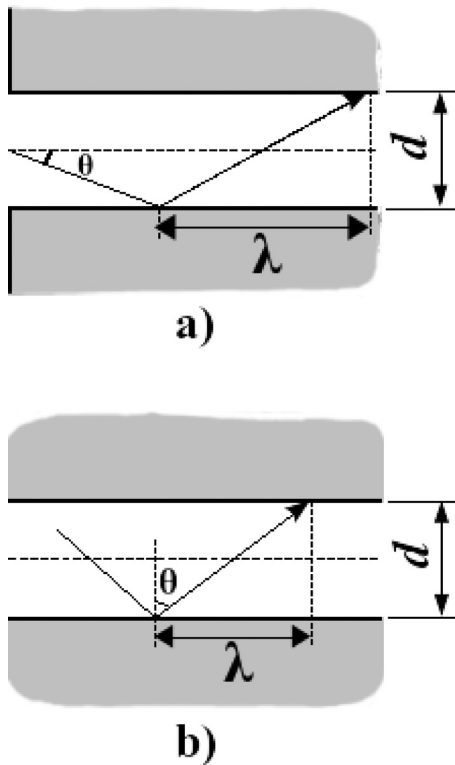


**FIG. 4.** Depiction of scattering events in nanotubes. (a) Specular reflection in the carbon nanotube leads to the scattering path length being determined by the entry angle of the particle as shown and being assigned a cosine-sine entry angle law. (b) For the non-carbon nanotube, the scattering path length is governed by diffuse reflection modeled by a cosine squared law with the angle defined as shown.

namely, we employ  $[\cos \theta \sin \theta]^2$ . Writing this in terms of the distance  $\lambda$  leads to

$$\cos^2[\arctan(d/\lambda)] \sin^2[\arctan(d/\lambda)], \tag{10}$$

where  $d$  is the pore diameter. Normalizing this over half space and using a trigonometric identity leads to

$$P_1(\lambda) = \frac{\pi d^3}{4 \left(1 + \frac{d^2}{\lambda^2}\right)^2} \lambda^2. \tag{11}$$

For the case of non-specular diffusion, it is assumed that the path length spectrum is determined by the particle-wall interaction and is assigned a cosine square law. Referring to Fig. 4(b), one finds that in this case  $\cos^2[\arctan(\lambda/d)]$ . Normalizing over half

space and using a trigonometric identity yields

$$P_2(\lambda) = \frac{d\pi}{2} \left[ \frac{1}{\left(1 + \frac{\lambda^2}{d^2}\right)} \right]. \tag{12}$$

The ratio  $J/J'$  can now be assembled.  $J'$  is proportional to the gaseous density gradient as in Sec. II, while  $J$  occurs at the constant density  $n_0$ . Nanotube diameters and collision frequencies are assumed equivalent. After canceling common factors, the flux ratio is assembled as

$$\frac{J}{J'} = \frac{\int_0^l \left( \int_z^\infty P_1(\lambda) d\lambda \right) dz}{(2/l) \int_0^{l/2} z \left( \int_z^\infty P_2(\lambda) d\lambda \right) dz}. \tag{13}$$

Upon using Eqs. (11) and (12) in Eq. (13) the inner integrals can be computed analytically leading to

$$\frac{J}{J'} = \frac{\int_0^l \frac{d^3 \pi}{16} \left[ \frac{\pi}{d} + \frac{2z}{d^2 + z^2} - \frac{2}{d} \arctan(z/d) \right] dz}{(2/l) \int_0^{l/2} z \frac{d^3 \pi}{4} \left[ \frac{\pi}{d} - \frac{2}{d} \arctan(z/d) \right] dz}. \tag{14}$$

The remaining integrals in Eq. (14) are computed numerically.

We let  $d = 1$  and give  $l$  units of pore diameter. A plot of the result is shown in Fig. 5. Here, we see a clear enhancement of the flow through the carbon based system over the traditional nanotube. The predicted flow enhancement continues to improve as the ratio  $l/d$  increases.

Considering the report of the flow enhancement of air through carbon nanotubes by Hotl *et al.*,<sup>2</sup> a range of multiples of the Knudsen prediction were given for three different membranes. Each of the three membranes used in this report was listed as having an identical range of pore diameters which average to 1.65 nm. Then, using the three membrane thicknesses listed, we are able to compute the ratio  $l/d$  for each of the Holt cases. This leads to  $l/d$  values of 1212, 1697, and 1818. Equation (14) predicts enhancements in the range of approximately 3.5 to 4 for this range of  $l/d$ .

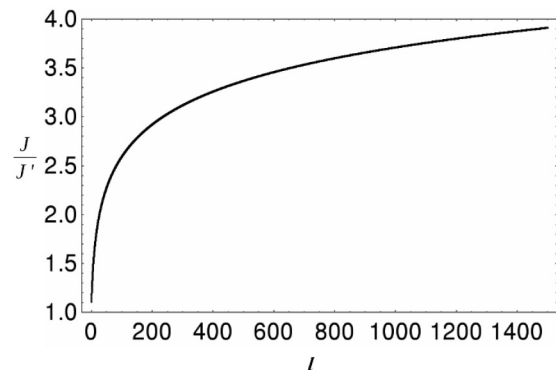


**FIG. 5.** Plot of Eq. (14) with  $l$  having units of pore diameter.

#### IV. CONCLUSION

In this report, it is demonstrated that a recently reported statistical model for gaseous flux in nanotubes can be used to arrive at analytic expressions that are used to predict and study the flow enhancement in carbon nanotubes. Results obtained are similar to those generated by complicated and time consuming MD simulations. This model gives the flux in terms of a probability distribution for scattering path lengths. Assuming that carbon nanotubes exhibit complete lack of friction for particle–wall interactions, the gaseous flow within this system is modeled as self-diffusion. The non-carbon nanotube system is assumed to exhibit perfectly diffuse transport style diffusion. To study the issue of the flow enhancement, the ratio of these two flux types is considered for two cases.

In the first case, both flux types are given a Gaussian scattering path length distribution. The flow enhancement is predicted to occur, and the magnitude of this enhancement is shown to vary with the standard deviation of the path length spectrum. As the standard deviation begins to broaden, and the distribution thus contains longer scattering path lengths, the enhancement factor goes from 3 asymptotically toward the value of 4. This result is consistent with results of the MD studies of Skoulidas *et al.*<sup>1</sup> on carbon nanotubes. Their simulations showed a self-diffusion enhancement over that of non-carbon based systems by a factor of 3 to 4 in rarefied situations for the gases CH<sub>4</sub> and H<sub>2</sub>. It is important to note that in this MD study the carbon nanotube was compared to a zeolite Si<sub>2</sub>O based system. Therefore, the flow enhancement predicted was for carbon nanotubes relative to zeolite pores. Additionally, self-diffusion and transport diffusion was considered in both materials. In the highly rarefied regime, the flow enhancements predicted for the carbon system over the zeolite appeared when self-diffusion was considered in both and also when transport diffusion was the transport mode in both. In this work, the enhancement was revealed when the carbon system had a self-diffusion flux while the non-carbon nanotube experienced transport diffusion but not when both systems had a transport diffusive flux.

As the distribution becomes dominated by increasingly shorter path lengths, the flow region enters an anomalous region where the enhancement diverges to increasingly larger values greater than 3. The enhancement values of 16–120 reported by Holt *et al.*<sup>2</sup> for airflow through carbon nanotubes could have occurred in this region. However, additional investigation is necessary in order to clarify such a speculation.

Additionally, we considered the case where the flux in each nanotube had its own peculiar path length spectrum. For the carbon nanotube with specular interactions, we modeled the scattering path length spectrum as being entirely determined by the trajectory of particles entering the pore opening. For the non-

carbon system with diffuse scattering, a cosine squared distribution is used to describe the scattering path length probability. Expressions for the flux in each case are developed and their ratios are investigated. In this case, the flow enhancement is given in terms of the pore length. For pores of the length used in Refs. 1 and 2, this method yields enhancement factors of 3 to 5. However, this result predicts that as the nanopore length increases beyond typical membrane thicknesses, the enhancement factor grows indefinitely. This is due to the fact that even though the transport flow in the non-carbon based system approaches a constant value for the tube of the infinite length, the self-diffusion flow in the carbon based tube continues to increase.

It is important to note that any effect due to the absorption of the gaseous species within the membrane was not considered in this study. Results from Ref. 1 seem to suggest that absorption of the gaseous species within the nanotube decreases the magnitude of gaseous self-diffusion. Thus, it is possible that gas absorption destroys the specular nature of the particle–wall collision within the carbon nanotube.

#### DATA AVAILABILITY

The data that support the findings of this study are available within the article.

#### REFERENCES

- <sup>1</sup>A. I. Skoulidas, D. M. Ackerman, J. K. Johnson, and D. S. Sholl, *Phys. Rev. Lett.* **89**(18), 185901 (2002).
- <sup>2</sup>J. K. Holt, H. G. Park, Y. Wang, M. Stadermann, A. B. Artyukhin, C. P. Grigoropoulos, A. Noy, and O. Bakajin, *Science* **312**, 1034 (2006).
- <sup>3</sup>B. J. Hinds, N. Chopra, T. Rantell, R. Andrews, V. Gavalas, and L. G. Bachas, *Science* **203**, 62 (2004).
- <sup>4</sup>J. Ramesh and C. R. Bertozzi, *Chem. Phys. Lett.* **494**, 1 (2010).
- <sup>5</sup>M. D. Yadav and K. Dasgupta, *Chem. Phys. Lett.* **748**, 137391 (2020).
- <sup>6</sup>J. M. De Sousa, P. A. S. Autreto, and D. S. Galvão, *Chem. Phys. Lett.* **739**, 136960 (2020).
- <sup>7</sup>D. G. Larrude, M. E. H. Maia da Costa, F. H. Monteiro, A. L. Pinto, and F. L. Freire, *J. Appl. Phys.* **111**, 064315 (2012).
- <sup>8</sup>K. Lafdi, A. Chin, N. Ali, and J. F. Despres, *J. Appl. Phys.* **79**, 6007 (1996).
- <sup>9</sup>D. Mantzalis, N. Asproulis, and D. Drikakis, *Chem. Phys. Lett.* **506**, 81 (2011).
- <sup>10</sup>D. Mantzalis, N. Asproulis, and D. Drikakis, *Chem. Phys. Lett.* **608**, 81 (2014).
- <sup>11</sup>A. Noy, H. G. Park, F. Fornasiero, J. K. Holt, C. P. Grigoropoulos, and O. Bakajin, *Nano Today* **2**, 22 (2007).
- <sup>12</sup>F. E. Colson and D. A. Barlow, *Phys. Rev. E* **100**, 062125 (2019).
- <sup>13</sup>R. L. Cunningham and R. J. J. Williams, *Diffusion in Gases and Porous Media* (Plenum Press, New York, 1980), pp. 8–13.
- <sup>14</sup>G. M. Turner, I. S. Falconer, B. W. James, and D. R. McKenzie, *J. Vac. Sci. Technol. A* **10**(3), 455 (1992).